

Modeling of Residual Stresses Induced in Machining Aluminum Magnesium Alloy (Al-3Mg)

O. Belgasim, M. H. El-Axir

Abstract--In order to achieve the desired surface integrity in a workpiece, it is important to select the correct cutting variables and the tool geometry. The influence of these measures on residual stresses induced in machining Aluminum Magnesium alloy (Al-3Mg) is investigated. Four input parameters are considered: cutting speed, feed rate, depth of cut and nose radius. The Response Surface Method was used to minimize the number of experiments to be conducted. Residual stresses were measured by electrochemical analysis by removing very fine layers of the machined surface. Experiments have shown that the residual stresses on the machined surface were often of the compressive type which tend to delay crack initiation and propagation that often tends to start from the machined surface itself.

Keywords: residual stresses; cutting variables; nose radius

I. INTRODUCTION

Metal cutting is still considered among the complex processes that require more research and investigation. The process output is highly dependent in input variables, since small variations in one of the input variables results in a considerable change in the output variables. The integrity of the surface produced in machining (process output) has recognized to have a significant impact on product performance and life time. Residual stress is a major component of surface integrity and is identified as a key factor that influences fatigue life, dimension accuracy and corrosion resistance of machined components.

The meaning of surface integrity can not be obtained in one dimension and does not depend only on surface roughness and geometry, but depends also on surface and substrate characteristics [1]. It includes elements describing the nature of surface and substrate, it also includes existence of micro-cracks, over-tempered martensite phase transformation and the residual stresses together with micro-hardness variation resulting from the machining process.

The majority of research work on residual stresses in metal cutting has been limited to experimental study [1-5] and others. Despite these efforts, the quantitative relationship between cutting conditions and residual stresses is still unknown due to the inherent complexity nature of the formation of residual stresses in metal cutting. A part of the recent research work in this field was based on the finite element models while others used different approaches to tackle the problem ranging from mathematical modeling to metallurgical investigations, etc.

Manuscript received October 8, 2009.

O. Belgasim is an associate professor at the Mechanical Engineering Department, Alfateh University, Tripoli, Libya

M. H. El-Axir is an associate professor at the Faculty of Engineering, Menoufia University, Egypt

The results presented by Wu and Matsumoto [6] show that material hardness has a direct and significant influence on the value of residual stress resulted by machining. They reported that since the method of machining hardened steel differs from that of machining soft steel, the machined surface of soft steel does not show any stage of phase transformation. Matsumoto and Barash [7] reported a case of reformation in machined surfaces of hardened steels and found that the residual stresses in soft steels are mostly tensile stresses while those remaining in hardened steels are mostly compressive stresses. The effect of high cutting speeds and feed rate on residual stresses on steel AISI 4340 has been investigated by Sadat [8]. He reported that the residual stresses on the surface are of the compressive type and they increase downwards below the surface to the maximum at a certain depth, then decrease any further below that depth. Another research which was conducted on two types of steel which have been machined by turning reported that residual stresses are influenced to a great extent by feed rate and nose radius, and to a certain extent by the cutting speed and the rake angle. Jang and others [9] investigated the effect of cutting variables (cutting speed, feed rate, depth of cut, geometry, and coating) on residual stresses in turning operations, they reported that residual stresses on stainless steel components are due to plastic deformation and thermal effect on tool nose. The results of the experiments conducted by Fuh [10] and Elkhabeery [11] show that the residual stresses of the tensile type is generated at the surface of many materials machined by milling in the presence of coolants. They also showed that maximum residual stress increases with an increase in feed rate, depth of cut and the tensile stress of the workpiece material.

This work studies the influence of cutting speed, feed rate, depth of cut, and nose radius of the cutting tool on residual stresses induced in the surface and substrate of aluminum magnesium alloy (Al-3Mg) when machined by precision turning operations. Cemented carbide tools of two different sizes (nose radius) are used. Turning operations were conducted by A CNC turning machine (Model, Biglia B56/1 CNC).

The results of this work will be presented to production engineers. It can be used as a useful guide to select the correct cutting variables and cutting tool particularly when the residual stresses induced in the work are a matter of concern.

II. EXPERIMENTAL WORK

Because of the wide application of aluminum magnesium alloys (Al-3Mg) in industry and being the material of many engineering components, it was used as a

test material in this work. The chemical composition in weight percent of the Aluminum alloy is shown in table I. The test material was received in the form of rings of outer diameter of 60 mm and inner diameter of 50 mm and 10 mm wide. Precision turning operations were done by the aid of mandrel specially made for the purpose of this work. In each set of tests one ring will be left without machining for the purpose of comparison.

Table I: Chemical composition of work material

Element	Zn	Cu	Si	Mg	Pb	Fe	Ti	Mn
Weight%	0.12	0.08	0.45	2.95	0.02	0.48	0.02	0.32

To study the effect of the precision machining on the induced residual stresses, three cutting variables were selected, namely: cutting speed (V), feed rate (f), and depth of cut (a_p). Turning operations were done by two types of cemented carbide inserts of two different nose radius. The values of the cutting variables and the types and geometry of cutting tools were presented in table II.

Table II: Summary of precision turning conditions

Cutting speed, V (m/min.)	218, 282, 377, 471, 535
Feed rate, f ($\mu\text{m}/\text{rev}$)	3, 10, 20, 30, 37
Depth of cut, a_p (μm)	8, 25, 50, 75, 92
Nose radius (mm)	0.4 mm and 0.8 mm
Cutting condition	Emulsified oil is used as coolant
Cutting tool material and dimensions	1) VBMT 16 04 04 – UM , C. Carbides 2) VBMT 16 04 08 – UM , C. Carbides
Effective tool angles	Rake = 4° , clearance = 6° , Entering angle = 75°
Tool holder code	SVJBL 2525 M16

The identification of residual stresses in the machined surface region was achieved in this work by the method of Deflection Etching Technique using electrochemical analysis. The electrochemical analysis method depends on the fact that the machined parts containing residual stresses will undergo shape variation due to removal of layers from the machined surface. The removal of external layers by electrochemical analysis results in elimination of part of the residual stresses which in turn leads to redistribution of the residual stresses to the equilibrium position which results in shape variation. This shape variation will be measured, and by then the angle of deviation of the residual stresses can be calculated.

When the precision machining on the ring is finished, the test specimen is prepared by drawing (marking) two parallel lines on the surface of the ring 5 mm apart and perpendicular to the periphery of the ring, then a third line perpendicular to the parallel lines is marked. The distance between the parallel lines along the perpendicular line is then measured.

By then the rings are cut or sheared in a position between the two parallel lines, this will result in elimination of a part of the residual stresses causing a change in ring circularity. The distance between the two parallel lines is measured once more, the change in reading of the distance can be either positive or negative depending on the type of

net residual stresses either being tensile or compressive stresses respectively. The ring is then sectioned into two parts in such a way that one of them is extended 5 mm beyond the line presenting the diameter of the ring. The three unmachined surfaces of the ring are coated with an isolating and corrosion resistance coating. The small section of the ring will be used for the determination of material removal rates. This is done by electrolytic analysis. The part is immersed in the electrolyte, as shown in Fig. 1., which shows the set-up of the apparatus prepared for this purpose. The part will be electrolytically etched. Etching is done in intervals of 5 minutes each. The decrease in the thickness is measured in each time, while the average thickness is found by weighing the specimen before and after etching. Etching can be done in a wide range of voltage and current, but the satisfactory conditions are achieved when 75 mg sodium chloride is dissolved in 1 liter of water at current density of 3.3 mA/mm.

The bigger section is used for determining the average residual stresses distribution. A magnification arm is attached to this part with a small mirror at the end, see Fig. 1. A laser pointer is used to measure angular deflection of the specimen while being etched, see Fig. 2. It is worth to mention that ring deflection consists of displacement and rotation components, but the application of this method enables measurement of rotation components only.

The residual stresses relieved due to the removal of a certain layer consists of three components thus: stresses relieved due to removal of n^{th} layer of metal, stresses relieved due to removal of previous layer, and stresses relieved due to initial cut of the ring. These stresses can be calculated as follows:

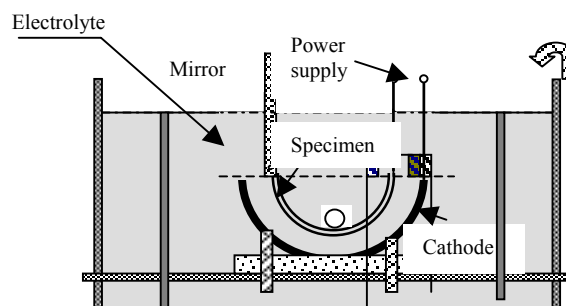


Fig. 1. Experimental set-up of the electrolytic dissolution of workpiece material

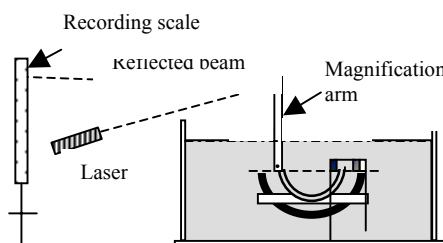


Fig. 2. Measurement of angular deflection of test specimen

1) stresses relieved due to removal of present layer

$$\sigma_{n,c} = \frac{Et^2 \varepsilon}{3\pi R dt} \dots\dots\dots(1)$$

Where E is modulus of elasticity, t is ring thickness, ε is angular rotation, R is ring radius.

2) stresses relieved due to removal of previous layers

$$\sigma_{n,p} = A[\Delta_n(4t_o - 4n\Delta t) - 2\Delta t(\Delta_{n-1} + \Delta_{n-2} + \dots + \Delta_2 + \Delta_1)]$$

Where A is ring deflection due to removal of n layers, t_o is initial ring thickness, Δt is change in thickness due to etching

3) stresses relieved due to initial sectioning of the ring

$$\sigma_{n,i} = \frac{\Delta D E}{2R^2} [z - \frac{t_o}{2}] \dots\dots\dots(3)$$

Where ΔD is the change in ring diameter due to initial sectioning, z is the remaining ring thickness, t_o is the initial ring thickness.

The total residual stresses relieved are then:

$$\sigma_{n,t} = \sigma_{n,c} + \sigma_{n,p} + \sigma_{n,i} \dots\dots\dots(4)$$

It is worth to mention that the calculated residual stresses are the stresses towards the periphery of the circle, the axial and radial components of residual stresses are in fact small enough and can be ignored.

III. EXPERIMENTAL DESIGN

The main objective of this work is to investigate the effect of the precision turning parameters (cutting conditions) on residual stresses generated in the work material. For the purpose of minimizing the experimental

work, a simple and adequate experimental design named response surface methodology (RSM), with the Box and Hunter method [12] is used. A detailed description of this method is presented elsewhere [13]. In this study, each parameter has five levels selected from practice, as shown in Table II. According to a central composite-second-order rotatable design with 3 independent variables, 20 experiments were conducted with the combination of values of cutting conditions, as shown in Table III.

The values of the levels of each cutting parameter used in this work were coded to simplify the experimental arrangement. The range of each parameter was also coded in five levels (-2, -1, 0, 1, 2) using the following transformation equations:

Cutting speed, $X_1 = \frac{V - V_0}{\Delta V}$, In the present work,

$$X_1 = \frac{V - 377}{94} \dots\dots\dots(5)$$

Feed rate, $X_2 = \frac{f - f_0}{\Delta f}$, In this work,

$$X_2 = \frac{f - 0.02}{0.01} \dots\dots\dots(6)$$

Depth of cut, $X_3 = \frac{a_p - a_{p0}}{\Delta a_p}$, In the present work,

$$X_3 = \frac{a_p - 0.05}{0.025} \dots\dots\dots(7)$$

Table IIIa: Experimental design (cutting variables)

Test No.	Speed (m/min)		Feed rate (mm/rev)		Depth of cut (mm)	
	Actual	coded	Act.	coded	Actual	coded
1	471	-1	0.01	-1	0.025	-1
2	282	+1	0.01	-1	0.025	-1
3	471	-1	0.03	+1	0.025	-1
4	282	+1	0.03	+1	0.025	-1
5	471	-1	0.01	-1	0.075	+1
6	282	+1	0.01	-1	0.075	+1
7	471	-1	0.03	+1	0.075	+1
8	218	+1	0.03	+1	0.075	+1
9	535	-1.682	0.02	0	0.05	0
10	218	+1.682	0.02	0	0.05	0
11	353	0	0.003	-1.682	0.05	0
12	377	0	0.037	+1.682	0.05	0
13	377	0	0.02	0	0.008	-1.682
14	377	0	0.02	0	0.092	+1.682
15	377	0	0.02	0	0.05	0
16	377	0	0.02	0	0.05	0
17	377	0	0.02	0	0.05	0
18	377	0	0.02	0	0.05	0
19	377	0	0.02	0	0.05	0
20	377	0	0.02	0	0.05	0

Table IIIb: Experimental results for both nose radii (r)

Test No.	SRS (MPa)		MRS (MPa)	
	r = 0.4	r = 0.8	r = 0.4	r = 0.8
1	-15	-42	120	-127
2	-90	-21	-120	-150
3	-8	-108	213	189
4	-30	-33	208	125
5	-100	-162	-142	-222
6	-75	-75	272	150
7	-60	-80	-185	30
8	-37	-44	258	150
9	-15	-160	-218	-212
10	-69	-36	-90	-103
11	-73	-80	-188	-270
12	-45	-58	110	--70
13	-15	-25	240	196
14	+105	-115	255	230
15	-45	-120	168	275
16	+45	-105	168	125
17	-30	-105	270	260
18	-42	-105	270	265
19	-37	-105	168	275
20	-37	-105	168	230

IV. MATHEMATICAL MODELS

By obtaining the results of residual stresses distribution, it is important to put the relation between surface and maximum residual stresses and the machining parameters in a mathematical form. Therefore, a mathematical model combining machining parameters and the residual stresses (RS) was generated as follows:

$$RS_{(0.4)} = -39.42 - 10.24 X_1 + 14.07 X_2 - 20.53 X_3 - 0.38 X_1^2 - 6.39 X_2^2 - 6.75 X_3^2 + 6.38 X_1 X_2 + 18.13 X_1 X_3 + 1.38 X_2 X_3 \dots \dots \dots (8)$$

$$RS_{(0.8)} = -107.7 + 31.2 X_1 + 5.1 X_2 - 22.7 X_3 + 4.8 X_1^2 + 15.1 X_2^2 + 14.7 X_3^2 - 0.6 X_1 X_2 + 3.6 X_1 X_3 + 24.1 X_2 X_3 \dots \dots \dots (9)$$

Mathematical models combining machining parameters with the maximum residual stress were also generated as follows:

$$MRS_{(0.4)} = 199.7 + 60.6 X_1 + 63.4 X_2 - 14.1 X_3 - 110.9 X_1^2 - 70.2 X_2^2 + 31.1 X_3^2 + 33.0 X_1 X_2 + 137.8 X_1 X_3 - 59.8 X_2 X_3 \dots \dots \dots (10)$$

$$MRS_{(0.8)} = 236.0 + 43.1 X_1 + 86.4 X_2 + 9.4 X_3 - 124.5 X_1^2 - 128.9 X_2^2 + 6.5 X_3^2 - 36.6 X_1 X_2 + 72.4 X_1 X_3 - 42.4 X_2 X_3 \dots \dots \dots (11)$$

Student's T-tests were done to determine the significant and non-significant coefficients. By omitting the non-significant coefficients the final equations for the mathematical models can be rewritten as follows:

Models for residual stresses on the surface (RS):

$$RS_{(0.4)} = -39.42 - 10.24 X_1 + 14.07 X_2 - 20.53 X_3 - 6.39 X_2^2 - 6.75 X_3^2 + 6.38 X_1 X_2 + 18.13 X_1 X_3 \dots \dots \dots (12)$$

$$RS_{(0.8)} = -107.7 + 31.2 X_1 + 5.1 X_2 - 22.7 X_3 + 4.8 X_1^2 + 15.1 X_2^2 + 14.7 X_3^2 + 24.1 X_2 X_3 \dots \dots \dots (13)$$

Models for maximum residual stresses (MRS):

$$MRS_{(0.4)} = 199.7 + 60.6 X_1 + 63.4 X_2 - 110.9 X_1^2 - 70.2 X_2^2 + 31.1 X_3^2 + 137.8 X_1 X_3 - 59.8 X_2 X_3 \dots \dots \dots (14)$$

$$MRS_{(0.8)} = 236.0 + 43.1 X_1 + 86.4 X_2 - 124.5 X_1^2 - 128.9 X_2^2 - 36.6 X_1 X_2 + 72.4 X_1 X_3 - 42.4 X_2 X_3 \dots \dots \dots (15)$$

The final models which were also tested by variance analysis (F-test) indicate that the adequacy of the model was established.

V. RESULTS AND DISCUSSION

Figures 3-5 show examples of the effect of various combinations of precision machining parameters (cutting speed, feed rate and depth of cut) on maximum residual stresses generated on the surfaces and parts of the substrate of Aluminum Magnesium alloy (Al-3Mg) workpieces that were machined either by inserts of nose radius $r=0.4$ mm or inserts of nose radius $r=0.8$ mm. The graphs were constructed from the experimental results using Response Surface Methodology (RSM) equations 14 and 15.

Each curve represents the effects of two input parameters while the other parameter was kept constant at a predetermined value.

A. Effect of cutting parameters

The effect of cutting speed on the maximum residual stress (MRS) for the two different nose radius inserts is shown in Fig.3. Different feed rates were used while

keeping the depth of cut constant at 0.05 mm. The trend of results in both cases are the same. However, high compressive residual stress are obtained when using tool nose radius of 0.8 mm as shown in Fig. 3b. Fig. 3 shows that the increase in cutting speed is associated with a decrease in the maximum compressive residual stresses, or a reversion into tensile stress. This is the case at any given values of feed rate. This can be attributed to metal softening and facilitated deformation of work material at elevated cutting speeds (Thermal effect). The rate of decrease of MRS is high at low feed rates and gets moderate to low at high feeds. Therefore higher feeds are more likely to cause tensile stresses. i.e. they are not favorable in this concern, since tensile stresses are not desirable as they can lead to cracking and fatigue.

The application of cutting tool of nose radius ($r = 0.4$ mm) leads to quite similar results at low cutting speeds till the compressive residual stresses reach the minimum or revert to tensile stresses. Further increases in cutting speed leads to increase in compressive residual stresses or to reversion of tensile stresses to compressive stresses.

It is worth to mention that surface residual stresses obtained for both cases of nose radius are compressive stresses which do not agree with those found by Matsumoto and Barash [7], this can be attributed to the different work material and low feed rates and depths of cut used in this work.

MRS is also influenced by the changes in depth of cut coupled with changes in cutting speed. Fig. 4 shows the effect of cutting speed on MRS for two different nose radius ($r = 0.4$ mm, $r = 0.8$ mm) at constant feed rate $f = 0.03$ mm/rev. Fig. 4a shows that the influence of the rate of change in MRS with the changes in cutting speed is lower at low values of depth of cut and gets higher with increasing depth of cut. It also shows that the change in MRS is always directly proportional to the cutting speed at high depth of cut, furthermore at certain cutting speeds the MRS reverts to tensile stresses. However, the case is quite different when cutting at low depth of cut, where the MRS increases with increasing cutting speed to a certain value then decreases by further increases in cutting speed.

With respect to the range of cutting conditions used in this work, it is evident that the maximum compressive residual stresses at both cases of nose radius ($r = 0.4$ mm and $r = 0.8$ mm) are at the lowest values of cutting speed and the highest depth of cut, see Fig. 4.

It is obvious that the values of MRS (compressive) were higher when cutting with nose radius ($r = 0.8$ mm), while the corresponding values of MRS when ($r = 0.4$ mm) is almost half the value. Therefore the magnitude of MRS is also sensitive to the nose radius of the cutting tool. The higher the nose radius of the tool the higher the magnitude of the MRS compressive induced in the workpiece.

The influence of depth of cut on the maximum residual stress at different feed rate is shown in Fig.5. For both cases of nose radius ($r=0.4$ and 0.8 mm) the effect of depth of cut on maximum residual stresses is not the same. In the case of low feed rates the maximum compressive residual stress decreases considerably with an increase in depth of cut. However, in the case of $r=0.4$ mm where there is an interaction between feed rates and depth of cut, It can be seen that at high feed rates the maximum compressive residual stress considerably increases as the depth of cut is increased.

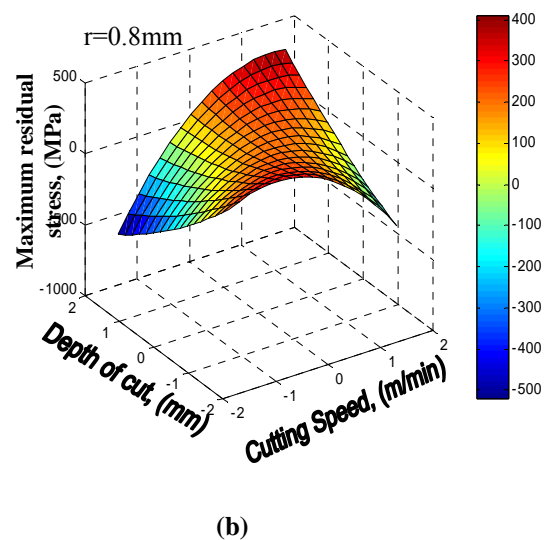
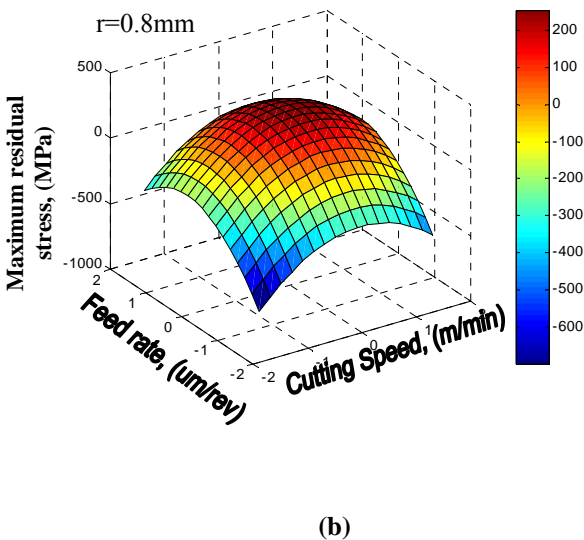
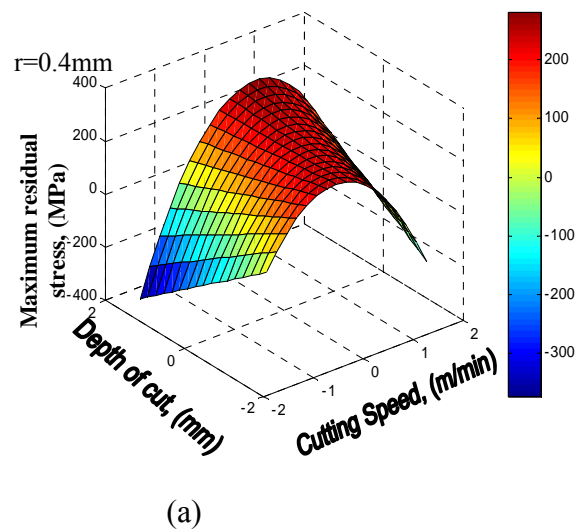
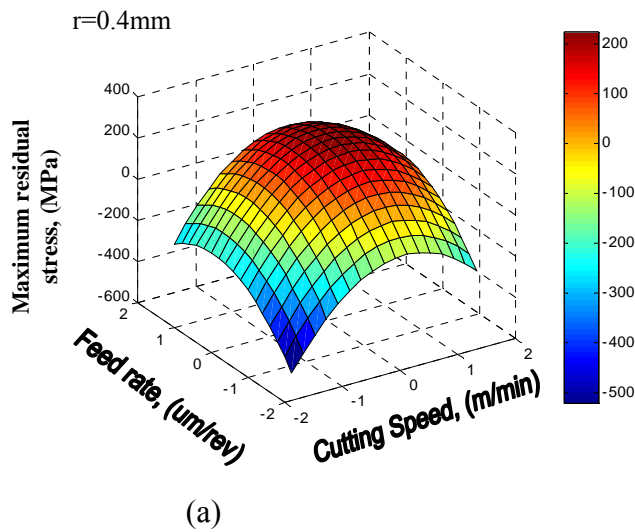


Fig. 4. Effect of cutting speed and depth of cut on maximum residual stress

Fig. 3. Effect of cutting speed and feed rate on maximum residual stress

It is often favorable to have compressive stresses in mechanical parts rather than tensile stresses as the compressive stresses play an important role in the function and service life of these parts, therefore it is eminent to set up the cutting conditions in the range which tends to induce compressive stresses in the work material avoiding conditions inducing tensile stresses as possible

VI. CONCLUSIONS

The present work has led to the following conclusions:

- 1- In the precision machining of Aluminum Magnesium Alloy (Al-3Mg) there is always a tendency of generation of both tensile and compressive residual stresses.
- 2- The analysis of variance has indicated that the second-order surface and maximum residual stress prediction models are adequate for the obtained experimental results.

- 3- The type of surface residual stresses induced in the machined surface of work material in both cases of nose radius 0.4mm and 0.8mm are compressive residual stresses.
- 4- The obtained results show that the maximum residual stresses can be either tensile or compressive according to cutting conditions.
- 5- Feed rate is the most significant parameter affecting maximum residual stress followed by cutting speed, then depth of cut.
- 6- The residual stresses are also sensitive to tool nose radius, the smaller the nose radius the lower the magnitude of the maximum compressive residual stress.
- 7- The type of residual stresses depends on the interfering effect between the mechanical effects and thermal effects during the machining operation.

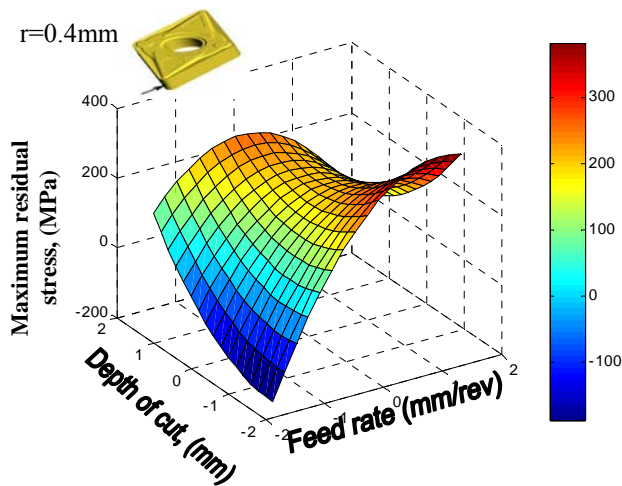


Fig. 5-a Effect of depth of cut and feed rate on maximum residual stresses (nose radius = 0.4 mm)

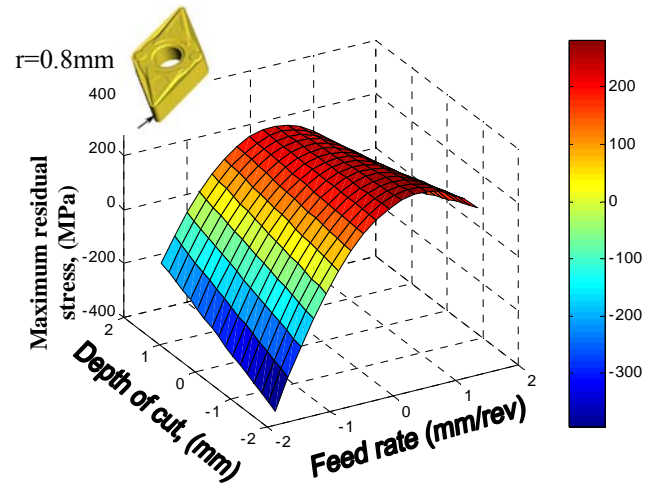


Fig. 5-b Effect of depth of cut and feed rate on maximum residual stresses (nose radius = 0.8 mm)

REFERENCES

- [1] Axinye, D. A.; Dewes, R. C.; "Surface integrity of hot work tool steel after high speed milling – Experimental data and Empirical models"; *Journal of Material Processing Technology*, Vol. 127, 325-335, 2000
- [2] Liu C. R., Barash M. M. ; "Variables governing patterns of mechanical residual stresses in a machined surface" *Trans. of ASME, Ser. B*, 104(3), 257-264, 1982
- [3] Konig W., Berktold A., Koch K. F. ; "Turning versus grinding – a comparison of surface integrity aspects and attainable accuracy" ; *CIRP Ann.*, 42 (1) ,39-43, 1993
- [4] Tonshoff H. K. , Wobker H. G., Brandt D. ; "Hard turning influences on the workpiece properties " *Trans. MAMRI/SME*, 23, 215-220, 1995
- [5] Ahga, H.; "Experimental study of surface roughness and residual stress in finish machining hardened steel " M. Sc. Thesis , School of industrial engineering, Purdue University, 1996
- [6] Wu, D. W.; Matsumoto, Y.; "The effect of hardness on the residual stresses in orthogonal machining of AISI 4340 steel" *Trans. ASME Journal of Engineering for Industry*, Vol. 112 (3) , pp. 245-252, 1990.
- [7] Matsumoto, Y. ; Barash, M., M. ; "Effect of hardness on surface integrity of AISI 4340 steel"; *Trans. of ASME, Journal of Engineering for Industry*, Vol. 108, pp 116-126, 1986
- [8] Sadat, A. B. "Effect of high speed turning of on surface integrity of 4340 steel"; *Journal of Material Science and Technology*, Vol. 9, pp. 371-375, 1990
- [9] Jang, D. Y.; Watkins, T. R., Kozack, K. J. "Surface residual stresses in machined austenitic stainless steel", *Wear Journal*, Vol. 194, pp. 168-173, 1996
- [10] Fuh, K. H.; Wu, C. F.; " A residual stress model for the milling of Aluminum alloy 2014-T6"; *Journal of Material Processing Technology*, Vol. 51, pp. 87-105, 1995.
- [11] El-Khabeery, M. M., Fattouh, M.; "Residual stress distribution caused by milling"; *International journal of machine tool and manufacture*, Vol. 29 (3), 00. 391-401, 1989.
- [12] Box, G. E. P.; Hunter, J. S.; "Multifactor experimental designs" *Ann. Math. Stat.* 28, 195.; 1957
- [13] Das, M. N.; Giri , N. G.; "Design and Analysis of Experiments"; 2nd edition, John Wiley, 1957